bioRxiv preprint doi: https://doi.org/10.1101/2021.04.26.441409; this version posted April 26, 2021. The copyright holder for this preprint (which was not certified by peer review) is the author/funder. All rights reserved. No reuse allowed without permission.

1 **Isolation and characterization of barley (*Hordeum vulgare*) extracellular vesicles and their**
2 **role in RNAi-based crop protection**

3 Schlemmer T[1,2], Weipert L[1], Preußer C[3], Hardt M[4], Möbus A[4], Barth P[5], Busche T[6], Koch A[2]

4 [1]Institute of Phytopathology, Centre for BioSystems, Land Use and Nutrition, Justus Liebig
5 University, Heinrich-Buff-Ring 26, D-35392, Giessen, Germany

6 [2]Institute of Phytomedicine, University of Hohenheim, Otto-Sander-Strasse 5, D-70599,
7 Stuttgart, Germany

8 [3]Center for Tumor Biology and Immunology, Philipps University, Hans-Meerwein Straße 3,
9 D-35032, Marburg, Germany

10 [4]Biomedical Research Centre Seltersberg (BFS), Imaging Unit, Justus Liebig University,
11 Schubertstraße 81, D-35392, Giessen, Germany

12 [5]Institute of Bioinformatics and Systems Biology, Justus Liebig University, Heinrich-Buff-
13 Ring 58, D-35392, Giessen, Germany

14 [6]Centre for Biotechnology - CeBiTec, Bielefeld University, Universitätsstraße 25, D-33615,
15 Bielefeld, Germany

16 Correspondence to

17 Aline.Koch@uni-hohenheim.de

18 **Keywords:** plant EV, extracellular vesicles, RNA interference, RNAi, siRNA, dsRNA, RNA
19 spray, barley, *Fusarium graminearum*,

20

21

bioRxiv preprint doi: https://doi.org/10.1101/2021.04.26.441409; this version posted April 26, 2021. The copyright holder for this preprint (which was not certified by peer review) is the author/funder. All rights reserved. No reuse allowed without permission.

22 **Abstract**

23 The demonstration that spray-induced gene silencing (SIGS) can confer strong disease
24 resistance bypassing the laborious and time-consuming transgenic expression of double-
25 stranded (ds)RNA to induce gene silencing of pathogenic targets was groundbreaking.
26 However, future field applications will require fundamental mechanistic knowledge on dsRNA
27 uptake, processing, and its transfer. There is increasing evidence that extracellular vesicles
28 (EVs) mediate the transfer of transgene-derived small interfering (si)RNAs in host-induced
29 gene silencing (HIGS) applications. Here, we examined the role of EVs regarding the
30 translocation of sprayed dsRNA from barley (*Hordeum vulgare*) to the target fungus *Fusarium*
31 *graminearum*. We found barley EVs with 156 nm in size containing predominantly 21 and 19
32 nucleotide (nt) siRNAs starting with a 5'-terminal Adenine. Notably, barley EVs contain less
33 siRNA compared to EVs isolated from transgenic HIGS Arabidopsis plants. Together our
34 results further underpin mechanistic differences between HIGS and SIGS applications and a
35 minor role of EVs in SIGS.

36 **Introduction**

37 RNAi-based plant protection strategies represent a powerful tool to address the goals of the
38 European "farm to fork" strategy to reduce the usage of pesticide about 50% till 2030. As an
39 alternative to conventional pesticides, RNAi-based plant protection holds enormous potential
40 to prevent further drastic loss of biodiversity. Over the last two decades, more than 170 studies
41 have demonstrated the feasibility of controlling agronomically and horticulturally relevant plant
42 diseases by utilizing transgenic expression (host-induced gene silencing [HIGS][1]) and
43 exogenous application (spray-induced gene silencing [SIGS][2]) of double-stranded RNA
44 (dsRNA) to trigger post-transcriptional gene silencing of target genes in various plant pathogens
45 and pests[3]. In addition to the academic proof-of-concept for numerous pathosystems, RNAi
46 technology has further advanced to enable lab-to-field transitions (e.g., costs, risk-assessment,

bioRxiv preprint doi: https://doi.org/10.1101/2021.04.26.441409; this version posted April 26, 2021. The copyright holder for this preprint (which was not certified by peer review) is the author/funder. All rights reserved. No reuse allowed without permission.

47 formulations, and regulations). Despite such significant achievements, however, we still lack a
48 mechanistic understanding of these technologies. For example, the mechanisms underlying the
49 transfer and uptake of transgene- or spray-derived RNAs during plant-fungal interactions
50 remain ill-defined, yet they play a pivotal role in determining efficacy and specificity for RNAi-
51 based plant protection. We predict that closing these gaps in knowledge will facilitate the
52 development of novel integrative concepts, precise risk assessment, and tailor-made RNAi
53 therapy for plant diseases. To this end, we assessed the role of extracellular vesicles (EVs) in
54 the transfer of SIGS-inducing RNAs.

55 Recent data suggest that, analogous to the role of mammalian exosomes in cell-to-cell
56 communication, fungi rely on a bidirectional sRNA transport system via EVs[4]. It has been
57 shown that EVs purified from *Arabidopsis thaliana* leaf extracts and apoplastic fluids contain
58 transgene-derived small interfering RNAs (siRNAs). Furthermore, RNA sequencing (RNA-
59 seq) analysis reveals that EVs from plants expressing CYP3RNA, a 791 nucleotide (nt) long
60 dsRNA originally designed to target the three *CYP51* genes of the fungal pathogen *Fusarium*
61 *graminearum* (*Fg*), contain CYP3RNA-derived small interfering RNAs (siRNAs)[5]. Notably,
62 the EVs' cargo retained the same CYP3RNA-derived siRNA profile as that of the respective
63 leaf extracts, suggesting no selective uptake of specific artificial sRNAs into EVs. Moreover,
64 mutants of the endosomal sorting complex required for transport-III (ESCRT-III) were
65 impaired in HIGS, and EVs were free of CYP3RNA-derived siRNAs[5]. The latter serves as
66 further indication that endosomal vesicle trafficking supports the transfer of transgene-derived
67 siRNAs between donor host cells and recipient fungal cells. Although the number of EV-
68 contained siRNAs was low, we lack information on the minimum concentration of siRNAs
69 required inside an EV to induce HIGS. Notably, we demonstrated previously that *Fg* can take
70 up long dsRNA that is processed by its own RNAi[6,7], which may explain why we observed
71 greater silencing efficacy of the fungal target genes[7]. Feeding on dead plant tissue, necrotrophic
72 fungi may take up topically-applied dsRNA or dsRNA that was delivered to the xylem[2].

bioRxiv preprint doi: https://doi.org/10.1101/2021.04.26.441409; this version posted April 26, 2021. The copyright holder for this preprint (which was not certified by peer review) is the author/funder. All rights reserved. No reuse allowed without permission.

73 Consequently, we speculate that the role of EVs is minor in the SIGS-*Fg*-barley system. In the
74 present study, we isolated, for the first time, EVs from dsRNA-sprayed barley leaves and
75 analyzed their RNA cargo to determine similarities and differences between EVs' RNA cargo
76 isolated by HIGS and SIGS strategies, respectively.

77 **Results and Discussion**

78 To study whether barley (*Hordeum vulgare*) EVs contain SIGS-derived RNAs, we established
79 a protocol for EV isolation from barley leaves by adjusting the EV isolation protocol we had
80 employed for *Arabidopsis* preparation[5]. Accordingly, unsprayed harvested leaf segments were
81 freshly cut on both ends immediately before being submerged in the vesicle isolation buffer.
82 The duration of vacuum infiltration was increased to four min and repeated three times to fully
83 infiltrate the barley leaves. In comparison, *Arabidopsis* leaves required only 1 min per round to
84 achieve full leaf infiltration. To harvest the apoplastic fluid, the centrifugation speed was
85 adapted from 700 xg to 1000 xg for 20 min at 4 °C. Purified barley EVs exhibited a highly
86 diverse size distribution with a mean size of 156 +/− 12.2 nm, which is slightly larger than the
87 mean size of EVs isolated from *Arabidopsis* (139 +/− 7.7 nm[5], Figs. 1a and 1b) but still fits
88 well within the standard 50–300 nm range for plant EVs[4]. Transmission electron microscopy
89 (TEM) revealed no obvious differences in electron density for barley EVs compared to
90 *Arabidopsis* EVs[5] (Fig. 1a). Notably, nanoparticle trafficking analysis (NTA) and TEM
91 displayed a strong heterogenicity of size among barley EVs compared to *Arabidopsis* EVs. In
92 addition, NTA revealed several peaks between 100 and 250 nm, which were confirmed by
93 TEM-based size measurements (Figs. 1a and 1b). However, additional verification is required
94 to confirm differences in EV biogenesis between monocot and dicot plant species. To our
95 knowledge, this is the first report on EVs isolated from barley leaves. Thus, we lack an EV
96 marker for immunodetection, which is necessary to prove the EVs' origin. For *Arabidopsis*
97 EVs, syntaxin PENETRATION1 (PEN1)[8] and TETRASPANIN8 (TET8)[9] are referenced EV

bioRxiv preprint doi: https://doi.org/10.1101/2021.04.26.441409; this version posted April 26, 2021. The copyright holder for this preprint (which was not certified by peer review) is the author/funder. All rights reserved. No reuse allowed without permission.

98 markers. Currently, the limited information on EV markers in *Arabidopsis* as the plant model
99 organism further impedes efforts to identify possible barley EV markers. Based on amino acid
100 similarity, we located 10 homologs for PEN1 and seven homologs for TET8 in barley (Figs. 1c
101 and 1d).

102 To verify the role of EV-mediated transport of SIGS-derived siRNA, barley leaves were
103 sprayed with CYP3RNA, as described[2]. EVs were isolated from apoplastic fluids, and EV RNA
104 cargos were examined by RNA-seq. sRNA-profiling of barley EVs revealed fewer CYP3RNA-
105 derived siRNAs (Fig. 1e), as the overall number of siRNAs that mapped to the CYP3RNA
106 precursor was lower than in both *Arabidopsis* samples[5]. Read coverage (number of reads that
107 overlapped at a certain position of the sequence) was also low (Fig. 1f). Notably, the siRNA
108 pattern demonstrated a bias towards siRNAs that matched the middle of the CYP3RNA triple
109 construct (Fig. 1g), which was observed for *Arabidopsis* as well[5]. Further analysis enabled the
110 identification of several of the same siRNAs in both systems, *Arabidopsis*-HIGS and barley-
111 SIGS. Our findings also indicate that the majority of siRNAs are 21 nt in length (Fig. 1h) and
112 preferentially start with an A (Fig. 1j), while siRNAs in EVs isolated from transgene-expressing
113 (HIGS) *Arabidopsis* plants begin with an A or U[5]. Based on sRNA-seq data revealing 5′-
114 identities and lengths of HIGS-derived siRNAs, we can speculate regarding contributing RNA-
115 binding proteins, insofar as they are known for the specific pathosystem. Interestingly, barley
116 EVs revealed a second peak for 19 nt siRNAs, which we did not observe in EVs from
117 *Arabidopsis* (Figs. 1h and 1i). This finding—along with previously discovered differences in
118 efficiencies between dsRNA originating from endogenous expression (HIGS) and dsRNA
119 originating from exogenous spray[10]—underlines mechanistic differences between HIGS and
120 SIGS regarding dsRNA uptake, processing, and transfer. In sum, our current knowledge
121 supports a model of HIGS that involves both plant Dicer-mediated processing of transgene-
122 derived dsRNA into siRNAs and ESCRT-III components mediating RNA transfer—possibly

bioRxiv preprint doi: https://doi.org/10.1101/2021.04.26.441409; this version posted April 26, 2021. The copyright holder for this preprint (which was not certified by peer review) is the author/funder. All rights reserved. No reuse allowed without permission.

123 via EVs. Nevertheless, the process by which EVs traverse the plant-fungal interface, as well as
124 the question of whether *Fg* takes up EVs or siRNA/dsRNA that is released from EVs prior to
125 uptake, remains unclear. In contrast, sprayed dsRNA is only partly processed by plant Dicers,
126 while unprocessed dsRNA was shown to be taken up by *Fg*[6,7]. This may explain the lower
127 amounts of siRNA in barley EVs compared to *Arabidopsis* EVs. However, future research must
128 determine whether the loading of unprocessed dsRNA into EVs contributes to SIGS.

129 When examined holistically, our data suggest that EV loading with CYP3RNA-derived siRNA
130 differs depending on whether HIGS and SIGS strategies are used. The data thus underline
131 mechanistic differences in the uptake and transfer mechanisms of siRNA/(dsRNA). Given these
132 differences, it is necessary to integrate our current knowledge regarding the molecular
133 properties (e.g., pathogen- or pest-specific RNAi mechanisms) with the related strengths and
134 limitations (e.g., routes of dsRNAs and siRNAs) of the chosen pathosystem. This information
135 must be considered when determining which HIGS/SIGS strategy is best.

136

137 **Material and Methods**

138

139 **Plant cultivation and CYP3RNA spray-application**

140 160 second leaves of barley cv. Golden Promise were harvested from plants growing for 3
141 weeks under long day conditions (16 h light, 22°C, 60% humidity). The leaves were transferred
142 to square petri dishes with 1% agar and divided into two groups. The upper part of the first
143 group were sprayed with CYP3RNA diluted in TE buffer and the second group was sprayed
144 with TE buffer as mock control as previously described[2] and incubated for 48 h before EV
145 isolation was performed.

146

147 **Negative staining and transmission electron microscopy (TEM)**

bioRxiv preprint doi: https://doi.org/10.1101/2021.04.26.441409; this version posted April 26, 2021. The copyright holder for this preprint (which was not certified by peer review) is the author/funder. All rights reserved. No reuse allowed without permission.

148 For TEM, copper formvar-coated 300-mesh electron microscopy grids were glow discharged
149 prior to sample application for 40 sec. Subsequently, 5 µl of the sample resuspended in PBS
150 were applied to the grids. Samples were dabbed off using Whatman filter paper and grids were
151 washed three times in 50 µl of 2% uranyl acetate and one time with distilled water. Needless
152 staining or fixing solutions, buffers and water were removed by Whatman paper between each
153 step. Finally, grids were air dried. Preparations were inspected at 120 kV under zero-loss
154 conditions (ZEISS EM912a/b) and images were recorded at slight underfocus using a cooled
155 2k x 2k slow-scan ccd camera (SharpEye / TRS) and the iTEM software package (Olympus-
156 SIS).
157
158 **Vesicle size and concentration measurements by nanoparticle trafficking analysis (NTA)**
159 For size and concentration prediction, purified barley EVs were diluted (1:50) with PBS.
160 Subsequently, 500 µL of vesicle suspension was loaded into Nanosight NS300 (Malvern
161 Panalytical). 5 measurements were performed at 25°C and size, concentration prediction and
162 statistical analysis were performed by the NTA 3.2 Dev Build 3.2.16 software.
163
164 **Determine siRNAs originating from CYP3RNA**
165 Vesicle RNA was isolated using the Single Cell RNA Purification Kit (Norgen Biotek)
166 according to the manufacturer's instructions described for cells growing in suspension. RNA
167 concentrations were determined using the NanoDrop spectrophotometer (Thermo Fisher
168 Scientific) and RNA was stored at -80°C before sending samples to RNA sequencing. Indexed
169 sRNA libraries were constructed from RNA isolated from vesicles with the TruSeq® Small
170 RNA Library Prep Kit (Illumina) according to the manufacturer's instructions. Indexed sRNA
171 libraries were pooled and sequenced on the Illumina MiSeq Platform (1 x 36 SE) and the
172 sequences were sorted into individual datasets based on the unique indices of each sRNA
173 library. The quality of the datasets was examined with FastQC (version 0.11.9)

bioRxiv preprint doi: https://doi.org/10.1101/2021.04.26.441409; this version posted April 26, 2021. The copyright holder for this preprint (which was not certified by peer review) is the author/funder. All rights reserved. No reuse allowed without permission.

174 (https://www.bioinformatics.babraham.ac.uk/projects/fastqc/) before and after trimming. The
175 adapters were trimmed using cutadapt (version 2.8)[11]. To filter out bacterial contaminations
176 kraken2 (version 2.1.1)[12] was used with the database obtained from the MGX metagenomics
177 application[13]. All reads marked as unclassified were considered to be of non-bacterial origin
178 and used for the subsequent alignment. The trimmed and filtered reads were mapped to the
179 CYP3RNA sequence using bowtie2 (version 2.3.2)[14] to identify siRNAs derived from the
180 precursor dsRNA sequence. The mappings were first converted into bedgraph using bedtools
181 (version 2.26.0)[15] and then to bigwig using bedGraphToBigWig[16]. These files were used for
182 visualization with IGV[17]. Read coverage is defined as the number of reads that match at a certain
183 position of the sequence.
184

185 **Determine frequency of different RNA species**

186 To determine RNA species, reference genome and annotation of Hordeum Vulgare (IBSC v2 –
187 release 47) were downloaded from EnsemblPlants[18]. Adapter trimming of raw reads was done
188 with TrimGalore (version 0.6.4)
189 (https://www.bioinformatics.babraham.ac.uk/projects/trim_galore/) which used cutadapt
190 (version 2.8)[11]. In this process all reads which became shorter than 18 nt were filtered out.
191 Afterwards, nucleotides with a phred score below 20 and reads retaining less than 90% of their
192 nucleotides in this process were removed using FASTQ Quality Filter from the FASTX-toolkit
193 (version 0.0.14) (https://github.com/agordon/fastx_toolkit). The bacterial contaminations were
194 filtered out as demonstrated in the previous section. The remaining reads were aligned to the
195 reference genome using STAR (version 2.7.3a)[19]. The number of different RNA species was
196 examined in R (version 4.0.2) (R Core Team, 2020) using featureCounts from the package
197 Rsubread (version 2.2.5)[20]. featureCounts was run for each sample using the previously
198 downloaded annotations of Arabidopsis. Following RNA types were examined: "lncRNA",

bioRxiv preprint doi: https://doi.org/10.1101/2021.04.26.441409; this version posted April 26, 2021. The copyright holder for this preprint (which was not certified by peer review) is the author/funder. All rights reserved. No reuse allowed without permission.

199 "pre_miRNA", "mRNA", "ncRNA_gene", "rRNA", "snoRNA", "snRNA" and "tRNA". All
200 alignments that could not be assigned to a feature were considered as "not assigned".
201
202 **Fig. 1**
203 (a) Barley EVs were negatively stained onto cooper formvar meshes using 2% uranyl acetate.
204 (b) Next, 5 µL of purified EVs were diluted up to a volume of 500 µL. Vesicle suspension was
205 loaded into Nanosight NS300 (Malvern Panalytical). Five measurements were performed at 25°
206 C, and size, concentration prediction, and statistical analysis were performed using the NTA
207 3.2 Dev Build 3.2.16 software. (c)(d) *Arabidopsis thaliana* PEN1 (AT3G11820) and TET8
208 (AT2G23810) paralogs of *Hordeum vulgare* subsp. vulgare were predicted by the NCBI's
209 protein BLAST service (https://blast.ncbi.nlm.nih.gov/Blast.cgi). (e) Relative amounts of
210 siRNAs isolated from Arabidopsis and barley EVs. (f) RNA was isolated from mock and
211 dsRNA-treated barley leaves. Indexed sRNA libraries were pooled and sequenced on the
212 Illumina MiSeq Platform (1 x 36 SE). The readings were then mapped onto the CYP3RNA
213 sequence. (g) Number of reads aligned to each CYP3RNA fragment (*CYP51A*, *CYP51B*,
214 *CYP51C*) were counted or (h) sorted based on their size. (i) siRNA size distribution of barley
215 EVs were compared with siRNA size distribution of *Arabidopsis* EVs. (j) The nucleotide
216 distribution for every position was counted for the 21 nt long siRNAs with perfect
217 complementarity towards the CYP3RNA precursor.
218
219 **Author Contributions**
220 T.S., L.W. and A.K. wrote the manuscript; A.K. and T.S. designed the study; T.S., and L.W.,
221 conducted the experiments; T.S., L.W., A.K., and P.B. analyzed all data and drafted the figures.
222 T.B. conducted RNA-seq experiments and T.B., and P.B. performed bioinformatics analysis.
223 All authors reviewed the final manuscript.
224

bioRxiv preprint doi: https://doi.org/10.1101/2021.04.26.441409; this version posted April 26, 2021. The copyright holder for this preprint (which was not certified by peer review) is the author/funder. All rights reserved. No reuse allowed without permission.

225 **Acknowledgements**

226 We thank C. Birkenstock and U. Schnepp for excellent plant. cultivation and M.Sc. C. Pfafenrot
227 and M.Sc. M. Mosbach for helping with the NTA measurements. This work was supported by
228 the Deutsche Forschungsgemeinschaft, Research Training Group (RTG) 2355 (project number
229 325443116) to AK and TS. We acknowledge access to compute resources of the Bielefeld-
230 Gießen Center for Microbial Bioinformatics (BiGi) financially supported by the BMBF grant
231 FKZ 031A533 within the de.NBI network.

232 **Competing financial interests**

233 The authors declare no competing financial interests.

234

235 **References**

236 1. Nowara, D. *et al.* HIGS: host-induced gene silencing in the obligate biotrophic fungal
237 pathogen Blumeria graminis. *The Plant cell* **22,** 3130–3141; 10.1105/tpc.110.077040
238 (2010).

239 2. Wang, M. & Jin, H. Spray-Induced Gene Silencing: a Powerful Innovative Strategy for Crop
240 Protection. *Trends in microbiology* **25,** 4–6; 10.1016/j.tim.2016.11.011 (2017).

241 3. Koch, A. & Wassenegger, M. Host-induced gene silencing - mechanisms and applications.
242 *The New phytologist*; 10.1111/nph.17364 (2021).

243 4. Rutter, B. D. & Innes, R. W. Extracellular vesicles as key mediators of plant-microbe
244 interactions. *Current opinion in plant biology* **44,** 16–22; 10.1016/j.pbi.2018.01.008 (2018).

245 5. Timo, S. *et al. Host-induced gene silencing involves Arabidopsis ESCRT-III pathway for*
246 *the transfer of dsRNA-derived siRNA* (2020).

bioRxiv preprint doi: https://doi.org/10.1101/2021.04.26.441409; this version posted April 26, 2021. The copyright holder for this preprint (which was not certified by peer review) is the author/funder. All rights reserved. No reuse allowed without permission.

247 6. Koch, A. *et al.* An RNAi-based control of Fusarium graminearum infections through
248 spraying of long dsRNAs involves a plant passage and is controlled by the fungal silencing
249 machinery. *Public Library of Science* **12** (2016).

250 7. Gaffar, F. Y., Imani, J., Karlovsky, P., Koch, A. & Kogel, K.-H. Different Components of
251 the RNA Interference Machinery Are Required for Conidiation, Ascosporogenesis,
252 Virulence, Deoxynivalenol Production, and Fungal Inhibition by Exogenous Double-
253 Stranded RNA in the Head Blight Pathogen Fusarium graminearum. *Frontiers in*
254 *microbiology* **10,** 1662; 10.3389/fmicb.2019.01662 (2019).

255 8. Rutter, B. D. & Innes, R. W. Extracellular Vesicles Isolated from the Leaf Apoplast Carry
256 Stress-Response Proteins. *Plant physiology* **173,** 728–741; 10.1104/pp.16.01253 (2017).

257 9. Cai, Q. *et al.* Plants send small RNAs in extracellular vesicles to fungal pathogen to silence
258 virulence genes. *Science (New York, N.Y.)* **360,** 1126–1129; 10.1126/science.aar4142
259 (2018).

260 10. Höfle, L. *et al.* Study on the efficiency of dsRNAs with increasing length in RNA-based
261 silencing of the Fusarium CYP51 genes. *RNA biology* **17,** 463–473;
262 10.1080/15476286.2019.1700033 (2020).

263 11. Martin, M. Cutadapt removes adapter sequences from high-throughput sequencing reads.
264 *EMBnet j.* **17,** 10; 10.14806/ej.17.1.200 (2011).

265 12. Wood, D. E., Lu, J. & Langmead, B. Improved metagenomic analysis with Kraken 2.
266 *Genome biology* **20,** 257; 10.1186/s13059-019-1891-0 (2019).

267 13. Jaenicke, S. *et al.* Flexible metagenome analysis using the MGX framework. *Microbiome*
268 **6,** 76; 10.1186/s40168-018-0460-1 (2018).

269 14. Langmead, B. & Salzberg, S. L. Fast gapped-read alignment with Bowtie 2. *Nature methods*
270 **9,** 357–359; 10.1038/nmeth.1923 (2012).

bioRxiv preprint doi: https://doi.org/10.1101/2021.04.26.441409; this version posted April 26, 2021. The copyright holder for this preprint (which was not certified by peer review) is the author/funder. All rights reserved. No reuse allowed without permission.

271 15. Quinlan, A. R. & Hall, I. M. BEDTools: a flexible suite of utilities for comparing genomic
272 features. *Bioinformatics (Oxford, England)* **26,** 841–842; 10.1093/bioinformatics/btq033
273 (2010).

274 16. Kent, W. J., Zweig, A. S., Barber, G., Hinrichs, A. S. & Karolchik, D. BigWig and BigBed:
275 enabling browsing of large distributed datasets. *Bioinformatics (Oxford, England)* **26,**
276 2204–2207; 10.1093/bioinformatics/btq351 (2010).

277 17. Thorvaldsdóttir, H., Robinson, J. T. & Mesirov, J. P. Integrative Genomics Viewer (IGV):
278 high-performance genomics data visualization and exploration. *Briefings in bioinformatics*
279 **14,** 178–192; 10.1093/bib/bbs017 (2013).

280 18. Howe, K. L. *et al.* Ensembl Genomes 2020-enabling non-vertebrate genomic research.
281 *Nucleic acids research* **48,** D689-D695; 10.1093/nar/gkz890 (2020).

282 19. Dobin, A. *et al.* STAR: ultrafast universal RNA-seq aligner. *Bioinformatics (Oxford,*
283 *England)* **29,** 15–21; 10.1093/bioinformatics/bts635 (2013).

284 20. Liao, Y., Smyth, G. K. & Shi, W. The R package Rsubread is easier, faster, cheaper and
285 better for alignment and quantification of RNA sequencing reads. *Nucleic acids research*
286 **47,** e47; 10.1093/nar/gkz114 (2019).

287

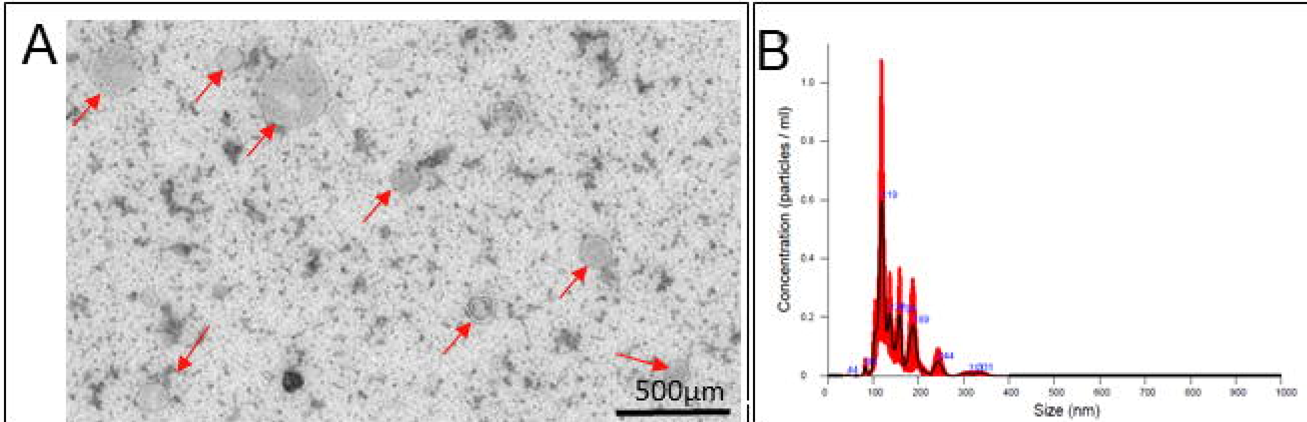
A
500µm
B
Concentration (particles / ml)
Size (nm)

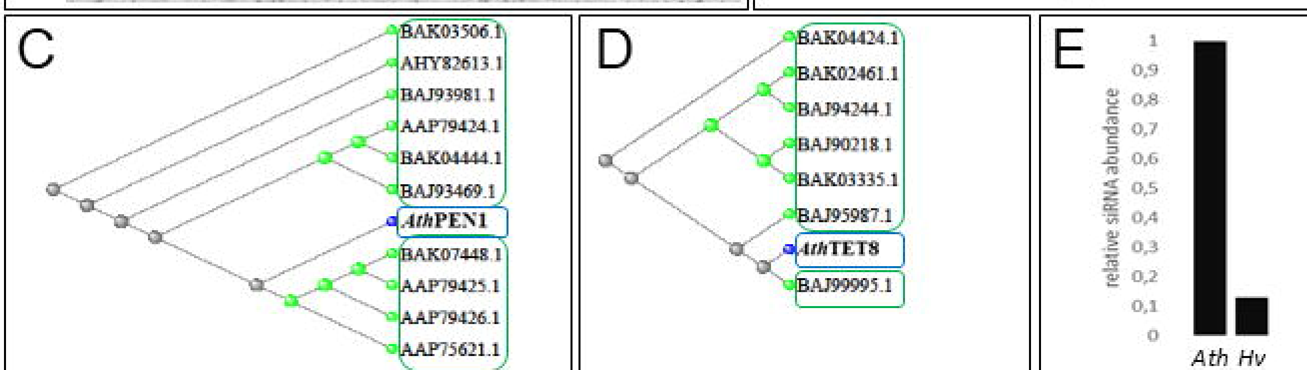
C
BAK03506.1
AHY82613.1
BAJ93981.1
AAP79424.1
BAK04444.1
BAJ93469.1
AthPEN1
BAK07448.1
AAP79425.1
AAP79426.1
AAP75621.1
D
BAK04424.1
BAK02461.1
BAJ94244.1
BAJ90218.1
BAK03335.1
BAJ95987.1
AthTET8
BAJ99995.1
E
relative siRNA abundance
Ath
Hv

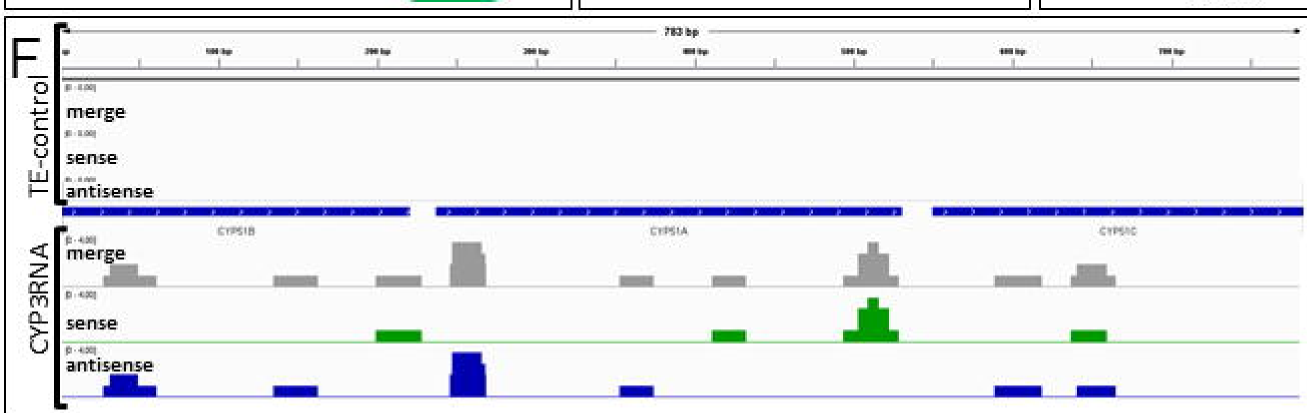
F
783 bp
TE-control
merge
sense
antisense
CYP51B
CYP51A
CYP51C
CYP3RNA
merge
sense
antisense

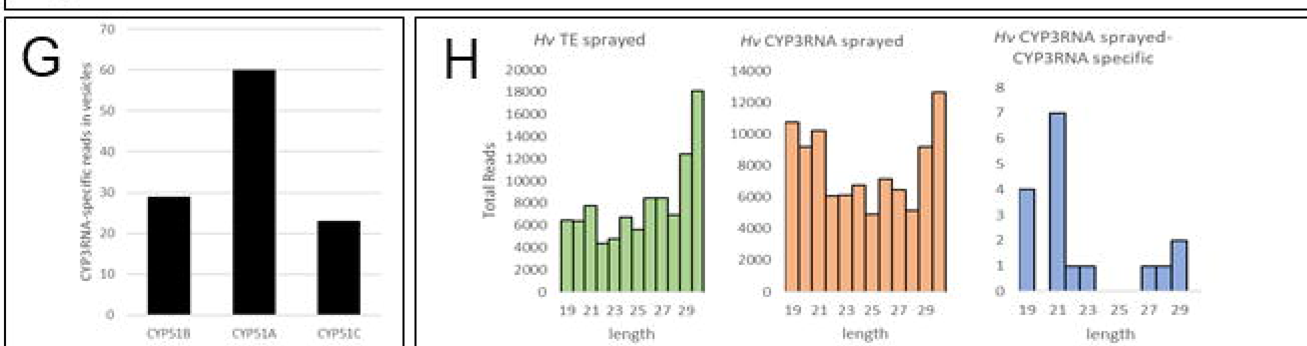
G
CYP3RNA-specific reads in vesicles
CYP51B
CYP51A
CYP51C
H
Hv TE sprayed
Hv CYP3RNA sprayed
Hv CYP3RNA sprayed-
CYP3RNA specific
Total Reads
length

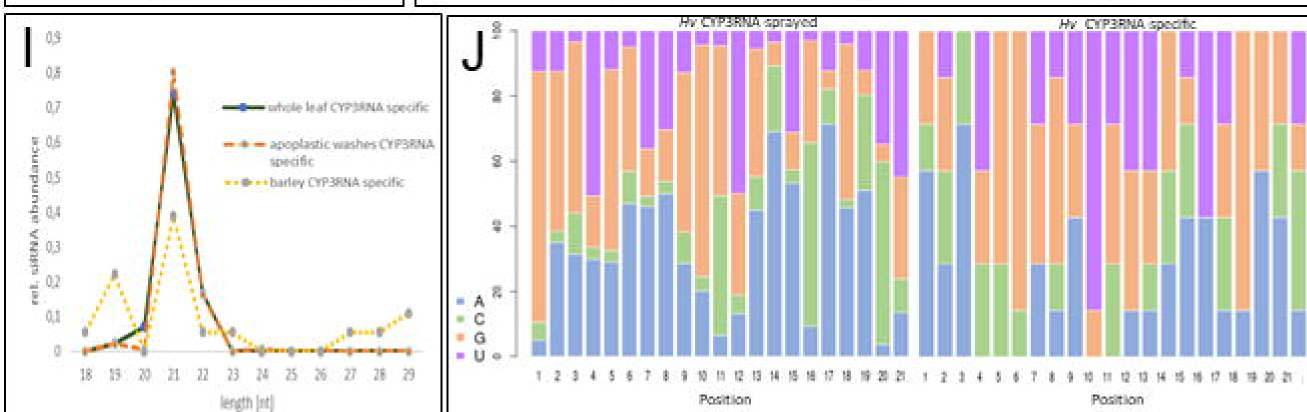
I
rel. siRNA abundance
whole leaf CYP3RNA specific
apoplastic washes CYP3RNA specific
barley CYP3RNA specific
length [nt]
J
Hv CYP3RNA sprayed
Hv CYP3RNA specific
A
C
G
U
Position